AIP | Applied Physics Letters

Onset of surface stimulated emission at 260 nm from AlGaN multiple quantum wells

Xiaohang Li, Hongen Xie, Fernando A. Ponce, Jae-Hyun Ryou, Theeradetch Detchprohm, and Russell D. Dupuis

Citation: Applied Physics Letters **107**, 241109 (2015); doi: 10.1063/1.4938136
View online: http://dx.doi.org/10.1063/1.4938136
View Table of Contents: http://scitation.aip.org/content/aip/journal/apl/107/24?ver=pdfcov
Published by the AIP Publishing

Onset of surface stimulated emission at 260 nm from AlGaN multiple quantum wells

Xiaohang Li,[1,2,a)] Hongen Xie,[3] Fernando A. Ponce,[3] Jae-Hyun Ryou,[4]
Theeradetch Detchprohm,[1] and Russell D. Dupuis[1,a)]
[1]*Center for Compound Semiconductors and School of Electrical and Computer Engineering, Georgia Institute of Technology, Atlanta, Georgia 30332, USA*
[2]*Computer, Electrical and Mathematical Sciences and Engineering Division, King Abdullah University of Science and Technology, Thuwal 23955, KSA*
[3]*Department of Physics, Arizona State University, Tempe, Arizona 85287, USA*
[4]*Department of Mechanical Engineering, Materials Science and Engineering Program, and Texas Center for Superconductivity at the University of Houston (TcSUH), University of Houston, Houston, Texas 77204, USA*

(Received 25 October 2015; accepted 6 December 2015; published online 18 December 2015)

We demonstrated onset of deep-ultraviolet (DUV) surface stimulated emission (SE) from *c*-plane AlGaN multiple-quantum well (MQW) heterostructures grown on a sapphire substrate by optical pumping at room temperature. The onset of SE became observable at a pumping power density of 630 kW/cm^2. Spectral deconvolution revealed superposition of a linearly amplified spontaneous emission peak at $\lambda \sim 257.0$ nm with a full width at half maximum (FWHM) of $\sim$12 nm and a superlinearly amplified SE peak at $\lambda \sim 260$ nm with a narrow FWHM of less than 2 nm. In particular, the wavelength of $\sim$260 nm is the shortest wavelength of surface SE from III-nitride MQW heterostructures to date. Atomic force microscopy and scanning transmission electron microscopy measurements were employed to investigate the material and structural quality of the AlGaN heterostructures, showing smooth surface and sharp layer interfaces. This study offers promising results for AlGaN heterostructures grown on sapphire substrates for the development of DUV vertical cavity surface emitting lasers (VCSELs). © *2015 AIP Publishing LLC*. [http://dx.doi.org/10.1063/1.4938136]

The development of III-nitride deep-ultraviolet (DUV) ($\lambda < 280$ nm) lasers has attracted considerable interest for important applications such as non-line-of-sight communication and biochemical detection. Recently, tremendous efforts have been made to demonstrate edge-emitting III-nitride DUV lasers with low thresholds and the shortest wavelength of 237 nm by optical pumping.[1–12] Achieving effective p-type doping in wide-bandgap III-nitride structures becomes a next critical step to realize the DUV laser diodes (LDs) by current injection.[13,14]

Bulk AlN and sapphire are two common substrates to grow wide-bandgap AlGaN heterostructures. The materials grown on the sapphire substrates generally suffer from high dislocation density due to large lattice and thermal mismatch in comparison to those grown on the AlN substrates. However, the use of sapphire substrates offers several benefits, such as low cost, large area, and little impurity absorption. Some of the aforementioned edge-emitting DUV lasers were demonstrated on the sapphire substrates.[1–4] These studies indicate that in spite of lattice and thermal mismatch, it is possible to obtain high internal quantum efficiency (IQE) and thus high material gain to achieve low-threshold lasing by reducing the dislocation density in III-nitride AlGaN heterostructures to a relatively low level.[15,16]

In comparison to the edge-emitting lasers, vertical-cavity surface-emitting lasers (VCSELs) possess advantageous characteristics including high-speed modulation, good beam quality, and control of production process. Despite decent progress of edge-emitting DUV lasers, little has been reported for the development of DUV VCSELs. Several additional breakthroughs are required to demonstrate DUV VCSELs. For example, VCSELs require distributed Bragg reflectors (DBRs) that are transparent to emitting photons with reflectivity close to unity. The reflectivity of current state-of-the-art III-nitride DUV DBRs is still limited to an insufficient level of $\sim$80%.[17,18] In addition, DUV surface stimulated emission (SE) from the III-nitride heterostructures needs to be demonstrated, which can be then matched to the resonant wavelength in the cavity provided by the high reflectivity DBRs. This was yet reported prior to this study.

In this work, we demonstrated onset of DUV surface SE at $\lambda \sim 260$ nm from AlGaN multiple-quantum well (MQW) heterostructures on a sapphire substrate by optical pumping at room temperature (RT). Epitaxial layers were grown by metalorganic chemical vapor deposition (MOCVD). Atomic force microscopy (AFM), scanning transmission electron microscopy (STEM), and power-dependent optical pumping measurements were performed to investigate the material and structural quality as well as luminescent characteristics.

A 20-nm low-temperature (LT) AlN buffer layer was first grown on a *c*-plane sapphire substrate at 960 °C, followed by an 800-nm high-temperature (HT) AlN template layer. An AlGaN MQW active region was grown on the AlN template layer at a relatively high temperature of 1250 °C to enhance the Al-atom mobility on the growing surface. The MQW structure comprises of ten periods of 2.1-nm $Al_{0.60}Ga_{0.40}N$ quantum wells (QWs) and 5.6-nm $Al_{0.78}Ga_{0.22}N$ quantum barriers (QBs). In addition, low V/III

[a)]Authors to whom correspondence should be addressed. Electronic addresses: xiaohang.li@kaust.edu.sa and dupuis@gatech.edu

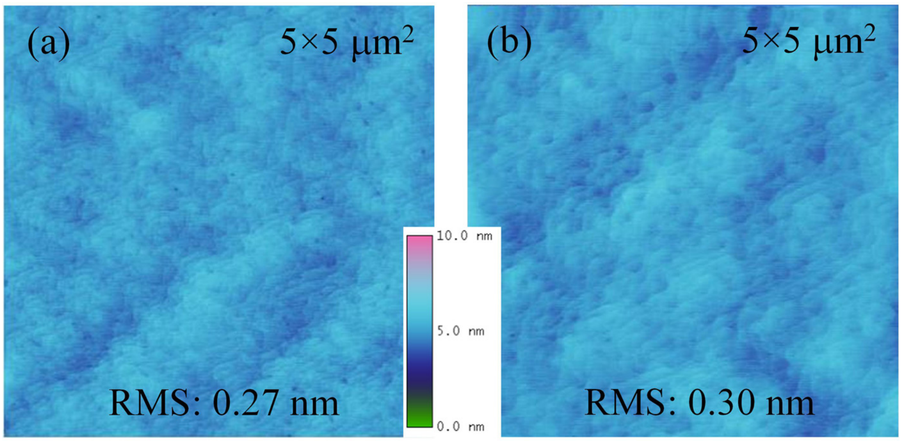

FIG. 1. AFM images and RMS roughnesses of the wafer (a) before and (b) after the growth of AlGaN MQW heterostructures.

ratios were individually optimized for the HT AlN template layer (V/III ∼ 30) and AlGaN MQW structure (V/III ∼ 50–100), which was found to promote two-dimensional growth and smooth surface formation. To obtain high-quality AlGaN MQWs, the epitaxial structure was grown using intentional interruption to switch the growth conditions between a QW and a QB. As the NH_3 flow rate was different between the QW and QB due to different V/III ratios, it was found that the NH_3 ramping time between the growths of the QW and the QB is influential on the luminescence characteristics. Zero or shorter ramping time can lead to a transient in the NH_3 flow rate, which resulted in uncontrollable inhomogeneity of material compositions and thus large full-width-at-half-maximum (FWHM) of the peak in the emission spectrum. On the other hand, longer ramping times caused a larger surface roughness due to the AlGaN decomposition at the high growth temperature of 1250 °C. Eventually, a ramping time of 2.5 s from the QW to QB and vice versa was found to be optimal.

AFM measurements were conducted to investigate surface morphology of the wafer before and after the growth of AlGaN MQWs, as shown in Figs. 1(a) and 1(b), respectively. As shown in Fig. 1(b), the root-mean-square (RMS) roughness of the wafer with the MQW active region was 0.30 nm. Considering that the AlN template layer showed a RMS roughness of 0.27 nm as exhibited in Fig. 1(a), the growth of the MQW structures resulted in minor surface roughening. In addition, the atomic step terrace profile was more profound in Fig. 1(b), suggesting good material and structural quality. These can be attributed to the growth of AlGaN MQWs at a relatively high temperature and hence higher Al mobility with optimized ramping time as mentioned above. Cross-sectional STEM analysis was carried on the wafer along a ⟨11–20⟩ projection, as shown in Fig. 2. Sharp and smooth QW/QB interfaces were observed and all the ten periods of uniform MQWs were present, which further supported good structural quality of the active region.

The optical pumping was employed to characterize the optical properties at RT. In the experimental setup, an ArF excimer laser provided a flat-top pumping beam at $\lambda = 193$ nm. A plurality of optical attenuators and mirrors were used to attenuate and redirect the pumping beam. An optical aperture was utilized to block the cross-sectionally inhomogeneous outskirt part of the pumping beam. The pumping beam fell onto the wafer surface perpendicularly. The pumping power density

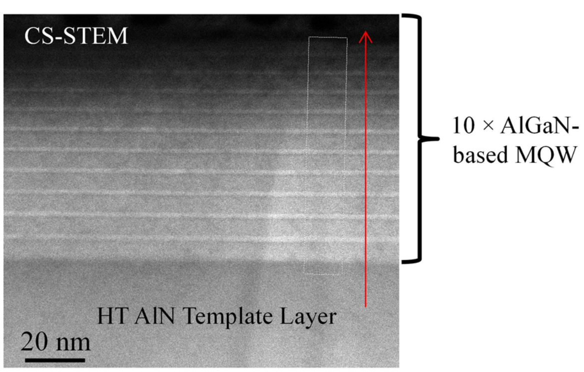

FIG. 2. A cross-sectional STEM image of the AlGaN MQW region.

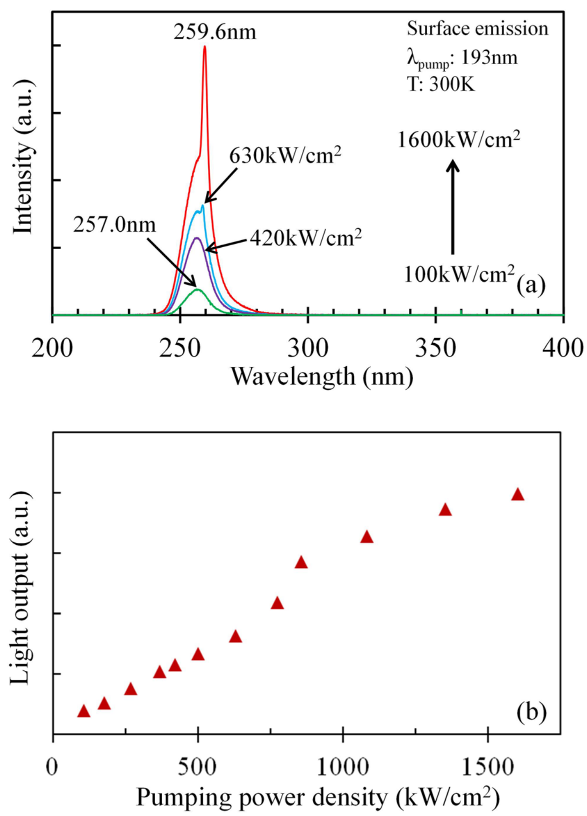

FIG. 3. (a) Surface emission spectra and (b) light output intensity of surface emission as a function of pumping power density.

was calculated by dividing output power of the pumping beam by the cross-sectional area of the beam. The photoluminescence (PL) emission was collected by an optical fiber. The fiber in use was a DUV-compatible Ocean-Optics fiber with a core size of 600 μm. It was about 45° tilted against the normal direction and 5 cm away above the wafer surface. The pumping power density was varied from 100 to 1600 kW/cm^2 during the measurement. As shown in Fig. 3(a), a spontaneous emission (SPE) spectrum with a peak wavelength of 257 nm was observed at low pumping power densities. As the power density increased, the onset of SE became observable at 630 kW/cm^2 with a peak wavelength of $\lambda \sim 260$ nm. With stronger pumping, the SE was further amplified. As shown in Fig. 4(b), the light output increased linearly at pumping power densities lower than 630 kW/cm^2. The light output then experienced a superlinear increase at 630–860 kW/cm^2, concurrently with the observation of the SE peak. This indicated a positive modal gain and amplification of SE.

To investigate the process of light amplification, peaks of the spectra taken at pumping power densities of 630–1600 kW/cm^2 were deconvoluted by using Gaussian fitting as shown in Figs. 4(a)–4(e). Each spectrum was normalized against the respective SE peak intensity. It is worth noting that it is difficult to accurately fit the spectra taken below 630 kW/cm^2. But it is appropriate to believe that the SE did not occur because of the existence of a single Gaussian-like peak and spectral similarity in that pumping range. As shown in Figs. 4(a)–4(e), the spectra comprised one broad SPE peak with a FWHM of $\sim$12 nm at $\lambda \sim 257$ nm. In addition, one narrow peak at $\lambda \sim 260$ nm with a FWHM of less than 2 nm was observed, which indicated the SE. The peak wavelength of SE was about 3-nm longer than that of the SPE. Similar shift was observed from some edge-emitting AlGaN DUV lasers before.[2,7] It is generally believed that in this situation the SE is caused by strong re-absorption of higher-energy photons and then emission and amplification of lower-energy photons from the SPE process collectively. Based on recent studies of SE from AlGaN heterostructures grown on *c*-plane sapphire substrates, the optical polarization of the SE at this wavelength is believed to be transverse-electric (TE) polarized.[1–3] The TE-polarized SE is ideal for emission extraction perpendicular from the wafer surface.[2] As the pumping power density increased, the relative intensities of SPE and SE peaks changed dramatically, suggesting continuous amplification of the SE. However, since the intensities of the two peaks were comparable at the largest pumping power density of 1600 kW/cm^2, the appearance of SE may not be considered as lasing where the amplification of SE should be so strong that it dominates the entire spectrum. Two factors may limit that from happening. First, the SPE and SE were not from a fabricated resonant

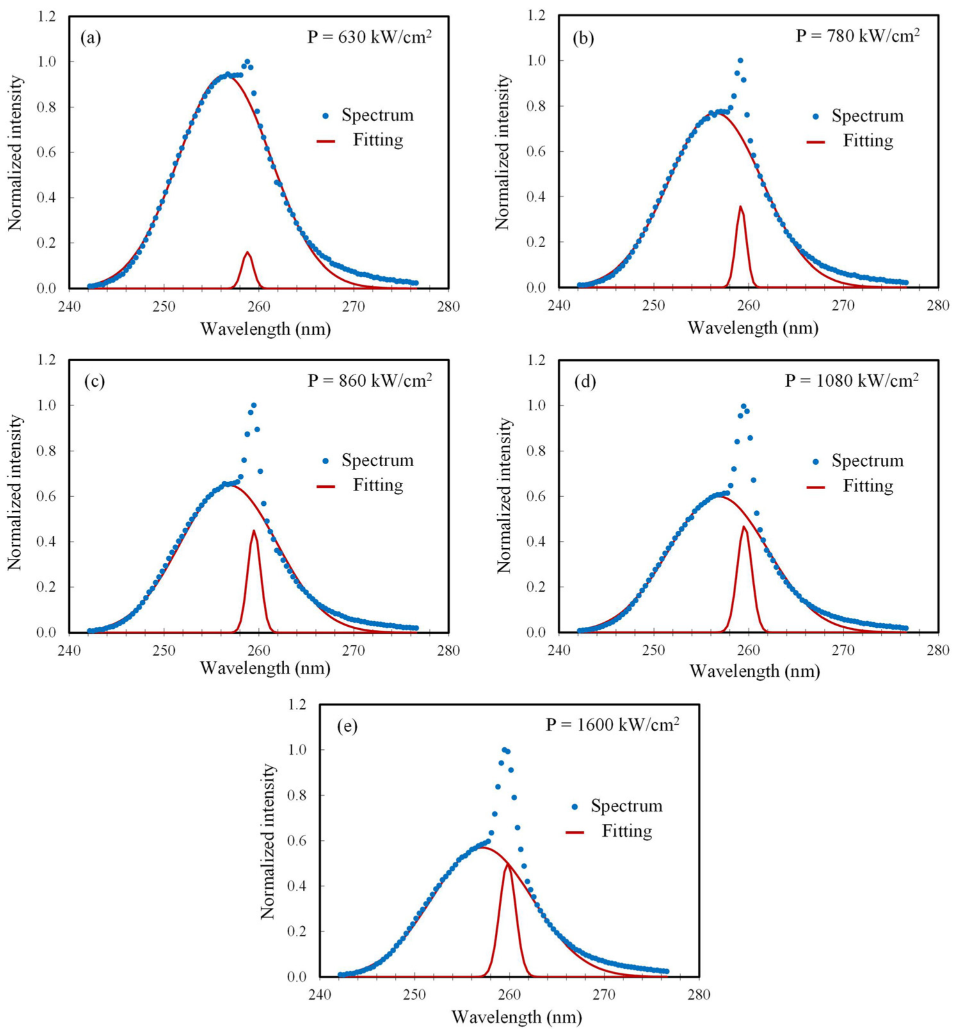

FIG. 4. (a)–(e) Spectra deconvoluted by Gaussian-fitting at different pumping power densities.

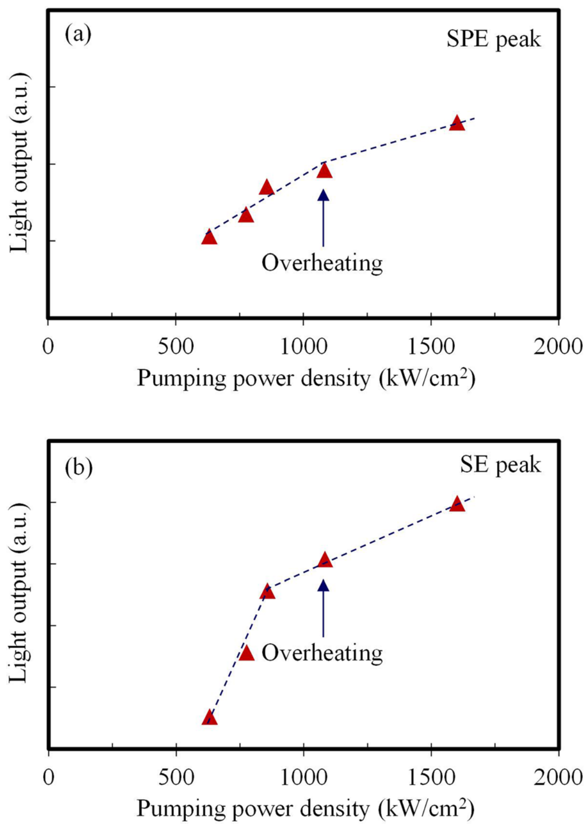

FIG. 5. Light outputs of (a) SPE and (b) SE peaks of the deconvoluted spectra (Figs. 4(a)–4(e)) at different pumping power densities.

cavity with highly reflective mirrors such as DBRs and a deliberate cavity thickness. Rather, it was obtained by optically pumping an unprocessed as-grown wafer. Second, the sapphire substrate has a low thermal conductivity of $\sim$35 W/(m·K). Thus, overheating could occur beyond a certain critical pumping power density. The overheating decreased IQE of the active region, thereby limiting strong amplification of SE.

As shown in Figs. 5(a) and 5(b), absolute light outputs of the SPE and SE peaks from Figs. 4(a)–4(e) were plotted as a function of the pumping power density, respectively. In Fig. 5(a), the light output of the SPE peak increased linearly with the pumping power density, which was consistent with the nature of SPE. However, the slope of linearity noticeably dampened at 1080 kW/cm^2 and above. In Fig. 5(b) on the other hand, it is noted that the light output of the SE peak increased rapidly with a large slope at 630–860 kW/cm^2, which represented the process of strong amplification of SE. But the slope also decreased at 1080 kW/cm^2 and above. The concurrent reduction of light output slopes of both SPE and SE peaks suggest that the reduced IQE as a result of overheating be the primary factor limiting the further strong amplification of SE. Further measures such as removal of sapphire substrate, installation of heat sink, and reduction of dislocation density can be taken to mitigate this issue for future development of DUV VCSELs.

In summary, the onset of DUV surface SE from AlGaN MQW heterostructures grown on a sapphire substrate was demonstrated at RT via optical pumping. The wavelength of $\sim$260 nm is the shortest for the surface SE from III-nitride MQW heterostructures to date, which indicates good material and structural quality due to the growth of AlGaN MQWs at a relatively high temperature of 1250 °C by MOCVD. This work offers promising results for the development of DUV VCSELs on inexpensive sapphire substrates.

X.H.L. acknowledges the support from the KAUST Startup and Baseline Funding. R.D.D. acknowledges the support from the Steve W. Chaddick Endowed Chair in Electro-Optics and the Georgia Research Alliance.

[1]X. H. Li, T. Detchprohm, T. T. Kao, Md. M. Satter, S. C. Shen, P. D. Yoder, R. D. Dupuis, S. Wang, Y. O. Wei, H. Xie, A. M. Fischer, F. A. Ponce, T. Wernicke, C. Reich, M. Martens, and M. Kneissl, Appl. Phys. Lett. **105**, 141106 (2014).
[2]X. H. Li, T. T. Kao, Md. M. Satter, Y. O. Wei, S. Wang, H. Xie, S. C. Shen, P. D. Yoder, A. M. Fischer, F. A. Ponce, T. Detchprohm, and R. D. Dupuis, Appl. Phys. Lett. **106**, 041115 (2015).
[3]J. Jeschke, M. Martens, U. Zeimer, A. Knauer, V. Kueller, C. Netzel, C. Kuhn, F. Krueger, C. Reich, T. Wernicke, M. Kneissl, and M. Weyers, IEEE Photonics Technol. Lett. **27**, 1969 (2015).
[4]S. V. Ivanov, D. V. Nechaev, A. A. Sitnikova, V. V. Ratnikov, M. A. Yagovkina, N. V. Rzheutskii, E. V. Lutsenko, and V. N. Jmerik, Semicond. Sci. Technol. **29**, 084008 (2014).
[5]Z. Bryan, I. Bryan, S. Mita, J. Tweedie, Z. Sitar, and R. Collazo, Appl. Phys. Lett. **106**, 232101 (2015).
[6]Y. S. Liu, Z. Lochner, T. T. Kao, Md. M. Satter, X. H. Li, J. H. Ryou, S. C. Shen, P. D. Yoder, R. D. Dupuis, Y. Wei, H. Xie, A. Fischer, and F. A. Ponce, Phys. Status Solidi C **11**, 258 (2014).
[7]W. Guo, Z. Bryan, J. Xie, R. Kirste, S. Mita, I. Bryan, L. Hussey, M. Bobea, B. Haidet, M. Gerhold, R. Collazo, and Z. Sitar, J. Appl. Phys. **115**, 103108 (2014).
[8]Z. Lochner, T. T. Kao, Y. S. Liu, X. H. Li, Md. M. Satter, S. C. Shen, P. D. Yoder, J. H. Ryou, R. D. Dupuis, Y. Wei, H. Xie, A. Fischer, and F. A. Ponce, Appl. Phys. Lett. **102**, 101110 (2013).
[9]T. Wunderer, C. Chua, Z. Yang, J. Northrup, N. Johnson, G. Garrett, H. Shen, and M. Wraback, Appl. Phys. Express **4**, 092101 (2011).
[10]J. Xie, S. Mita, Z. Bryan, W. Guo, L. Hussey, B. Moody, R. Schlesser, R. Kirste, M. Gerhold, R. Collazo, and Z. Sitar, Appl. Phys. Lett. **102**, 171102 (2013).
[11]N. M. Johnson, B. Cheng, S. Choi, C. L. Chua, C. Knollenberg, J. E. Northrup, M. R. Teepe, T. Wunderer, and Z. Yang, paper presented at the 9th International Symposium on Semiconductor Light Emitting Devices, Berlin, Germany, 23 July 2012.
[12]T. T. Kao, Y. S. Liu, Md. M. Satter, X. H. Li, Z. Lochner, J. H. Ryou, P. D. Yoder, T. Detchprohm, Y. Wei, H. Xie, A. Fischer, F. A. Ponce, R. D. Dupuis, and S. C. Shen, Appl. Phys. Lett. **103**, 211103 (2013).
[13]Y. S. Liu, T. T. Kao, Md. M. Satter, Z. Lochner, S. C. Shen, T. Detchprohm, P. D. Yoder, R. D. Dupuis, J. H. Ryou, A. M. Fischer, Y. O. Wei, H. Xie, and F. A. Ponce, IEEE Photonics Technol. Lett. **27**, 1768 (2015).
[14]Md. M. Satter, Z. Lochner, T. T. Kao, Y. S. Liu, X. H. Li, S. C. Shen, R. D. Dupuis, and P. D. Yoder, J. Quantum Electron. **50**, 166 (2014).
[15]X. H. Li, S. Wang, H. Xie, Y. O. Wei, T. T. Kao, Md. M. Satter, S. C. Shen, P. D. Yoder, T. Detchprohm, R. D. Dupuis, A. M. Fischer, and F. A. Ponce, Phys. Status Solidi B **252**, 1089 (2015).
[16]X. H. Li, Y. O. Wei, S. Wang, H. Xie, T. T. Kao, Md. M. Satter, S. C. Shen, P. D. Yoder, T. Detchprohm, R. D. Dupuis, A. M. Fischer, and F. A. Ponce, J. Cryst. Growth **414**, 76 (2015).
[17]L. Zhang, K. Dong, D. Chen, Y. Liu, J. Xue, H. Lu, R. Zhang, and Y. Zheng, Appl. Phys. Lett. **102**, 242112 (2013).
[18]G. Brummer, D. Nothern, A. Yu. Nikiforov, and T. D. Moustakas, Appl. Phys. Lett. **106**, 221107 (2015).